International Journal of Heat and Fluid Flow 68 (2017) 151–157

Contents lists available at ScienceDirect

International Journal of Heat and Fluid Flow

journal homepage: www.elsevier.com/locate/ijhff

An autonomous flexible propulsor in a quiescent flow

Boyoung Kim[a,1], Sung Goon Park[a,1], Wei-Xi Huang[b], Hyung Jin Sung[a,*]

[a] Department of Mechanical Engineering, KAIST, 291 Daehak-ro, Yuseong-gu, Daejeon 34141, Republic of Korea
[b] Department of Engineering Mechanics, Tsinghua University, Beijing 100084, China

ARTICLE INFO

Keywords:
Autonomous flexible propulsor
Ground effect
Penalty method
Immersed boundary method

ABSTRACT

Flapping motions of wings and fins are common in nature. Living organisms use such motions to float in a fluid or to propel themselves forward. Some entities, such as tadpoles, use distinct flexible components to generate propulsion. Here we introduce a propulsor consisting of a rigid circular head containing an energy source and a flexible fin for propulsion. The head imparts a sinusoidal torque to the leading edge of the fin and the flexible fin flaps along the leading edge. The flexible propulsor thus moves via an oscillating relative angle between the head and the leading edge of the fin. Unlike a self-propelled heaving and pitching fin, our 'autonomous' flexible propulsor has no prescribed motion or constraint referenced from outside coordinates. The immersed boundary method was used to model the interaction between the flexible propulsor and the surrounding fluid. A penalty method, in which the head and fin imparted a periodic torque to each other, was used to connect the head and the fin. The cruising speed and propulsive efficiency of the propulsor were explored as a function of the ratio of the head size to the fin length (D/L), the pitching amplitude (θ_p) and the pitching frequency (f). The cruising speed and the equilibrium position (g_{eq}) of the flexible propulsor near the ground were also examined. The optimal propulsive efficiency was achieved at the head ratio of $D/L = 0.2$ at $\theta_p = 30^\circ$ and $f = 0.2$. The cruising speed of the flexible propulsor increased when operating near the ground. The gap distance between the propulsor and the ground was dynamically determined by the pitching motion.

1. Introduction

Animals such as birds, insects, bats and fish use flapping motions of wings or fins to generate lift or thrust. Research in this area is motivated not only by the fundamental task of understanding the mechanisms underlying animal flight and swimming, but also by the desire to develop technologies such as micro air vehicles and autonomous underwater vehicles based on biomimetics (Borazjani and Sotiropoulous, 2009; Williams et al., 2014; McColgan and McGookin, 2015; Park and Sung, 2016; Fang et al., 2017). Analyses of fluid-structure interactions not only help us understand how fish, birds and cells move through fluids such as water, air and blood, they can also be used by researchers in biomimetic engineering, bioengineering and industrial engineering as a basis for new technologies. To explore the mechanism of efficient locomotion in animals, many researchers have performed theoretical (Lighthill, 1970; Wu, 1971; Moore, 2014), numerical (Kern and Koumoutsakos, 2006; Zhang et al., 2010; Zhu et al., 2014b; Park et al., 2014; Yeh and Alexeev, 2014; Kim et al., 2016; Park et al., 2016a) and experimental studies (Godoy-Diana et al., 2009; Thiria and Godoy-Diana, 2010; Quinn et al., 2014).

The propulsion force generated by flapping enables the swimmer to move across the streamlines. A microorganism is able to swim in a fluid by wiggling a flagellum due to an anisotropic hydrodynamic friction of a long and slender body (Elgeti et al., 2015). Zoettl and Stark (2012, 2013) showed that a self-propelled swimmer in a two-dimensional channel exhibits periodic stable oscillations around the centerline. These periodic trajectories are strongly influenced by random tumbling (Chilukuri et al., 2014) and the proximity of a rigid boundary (Berke et al., 2008; Drescher et al., 2011). Bacterial transport appears to be suppressed in a shear Poiseuille flow, leading to the depletion of swimmers at the center of the channel (Rusconi et al., 2014). Moore (2014) developed the small amplitude theory to model a flapping wing and observed a significant performance improvement when the wing was driven at a resonant frequency in the wing-fluid system. Numerical simulations of a self-propelled flapping system were conducted recently by several groups (Yeh and Alexeev, 2014; Zhu et al., 2014a,b; Kim et al., 2016), mainly focusing on the effects of flexibility on propulsive efficiency, cruising speed and wake symmetry. Despite these recent studies on self-propelled flexible propulsors, the excitation motion of such propulsors (usually the motion of the leading edge) is

* Corresponding author.
E-mail address: hjsung@kaist.ac.kr (H.J. Sung).
[1] Both authors contributed equally.

http://dx.doi.org/10.1016/j.ijheatfluidflow.2017.10.006
Received 1 May 2017; Received in revised form 26 September 2017; Accepted 18 October 2017

described in an external coordinate.

In studies of macro-scale biolocomotion, the effect of boundary confinement is also termed the ground or wall effect. This effect can be found in systems involving steady gliding with a fixed-wing configuration. For example, the black skimmer (*Rynchops nigra*) exploits the ground effect when gliding to increase its foraging efficiency (Withers and Timko, 1977). Gliding pelicans have also been found to achieve significant energy savings from the ground effect (Hainsworth, 1988). A similar aerodynamic advantage was found for flying fish gliding close to the sea surface (Park and Choi, 2010). The ground effect is also observed in systems undergoing undulatory swimming with a deforming body or fin. Quinn et al. (2014) used the unsteady potential flow method to compute the thrust and lift on a pitching aerofoil close to a solid boundary. In two other studies, viscous flow simulations were conducted to study the aerodynamic behavior of an inverted airfoil (based on the front wing of a Formula One car) oscillating near the ground (Molina et al., 2011; Moryossef and Levy, 2004). These works examined the role of the ground effect in the production of a downward force (negative lift force).

Recently, several extensive studies have examined flexible propulsors under the influence of the ground effect (Ryu et al., 2016; Dai et al., 2016; Tang et al., 2016). Tang et al. (2016) observed three regimes for a flexible plate near the ground; expensive, benefited and uninfluenced regimes. The propulsion speed increased and a larger amount of input work was required in the expensive regime. In the benefited regime, on the other hand, the input work decreased, increasing the efficiency. Park et al. (2017) modeled a flexible fin swimming near the ground and used a scaling analysis to investigate the ground effect. Both the thrust and the input power increased when operating near the ground as compared to far from the ground. The thrust increment was larger than that of the input power, leading to the improvement of the propulsive efficiency by the ground effect (Park et al., 2017). Most of these studies determined the propulsive efficiency and cruising speed with the propulsor positioned at a specific distance from the wall, because fixed or self-propelled fins cannot change direction.

The objective of the present work was to model an 'autonomous' flexible propulsor in a quiescent flow. Here, the term 'autonomous' was used to distinguish the propulsors which determined both the swimming direction and velocity 'autonomously' from those of which the direction or velocity was externally determined (prescribed). We were not aimed at creating a bio-inspired propulsor, but mainly proposed a basic numerical idea to generate propulsion by using two distinct components and analyzed the propulsion mechanism, which would be important for the macroscopic swimmers such as tadpoles. A rigid head was attached on a flexible fin to create a flexible propulsor. The propulsor was propelled via the relative pitching motion between the head and the fin. The fluid and body motions were solved independently and their interaction was realized by using the immersed boundary method. The motions of the head and fin were connected by adding a penalty force. A series of numerical simulations was carried out in which the physical parameters were varied. The cruising speed (U_c) and propulsive efficiency (η) of the propulsor were explored as a function of the ratio of the head size to the fin length (D/L), the pitching amplitude (θ_p) and the pitching frequency (f). The autonomous flexible propulsor could maneuver in response to the surrounding environment and its behavior near the ground was examined in terms of the cruising speed (U_c) and equilibrium position (g_{eq}).

2. Numerical method

Fig. 1(a) shows schematics of the flexible propulsor in a quiescent flow. The head diameter and the fin length are denoted by D and L, respectively. The leading edge of the flexible fin was hinged at the rear stagnation point of the circular head. The fluid motion was governed by the incompressible Navier–Stokes equations, which were non-

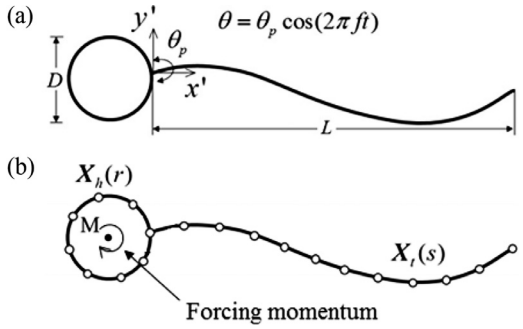

Fig. 1. Schematics of the (a) computational model and (b) configuration of the autonomous flexible propulsor. The reference frame of the head is denoted as *x'* and *y'* in (a).

dimensionalized by the reference velocity U_0 for the velocity vector $\boldsymbol{u} = (u, v)$, L/U_0 for the time t, $\rho_0 U_0^2$ for pressure p (where ρ_0 is the fluid density) and $\rho_0 U_0^2/L$ for the Eulerian momentum force $\boldsymbol{f}$,

$$\frac{\partial \boldsymbol{u}}{\partial t} + \boldsymbol{u}\cdot\nabla\boldsymbol{u} = -\nabla p + \frac{1}{\mathrm{Re}}\nabla^2\boldsymbol{u} + \boldsymbol{f}, \tag{1}$$

$$\nabla\cdot\boldsymbol{u} = 0, \tag{2}$$

where the Reynolds number is defined by $Re = \rho_0 U_0 L/\mu$ and μ is the dynamic viscosity (Huang et al., 2011). The dynamic viscosity of the fluid and the fin length were fixed and the reference velocity U_0 was determined by the specified Reynolds number. Eqs. (1) and (2) were solved by using the fractional step method with a staggered Cartesian grid system and the second-order accuracy was guaranteed in time for velocity and pressure (Park and Sung, 1995; Kim et al., 2002).

The governing equations for the inextensible flexible fin attached to the rigid circular head were non-dimensionalized by introducing the following characteristic scales: L/U_0 for the time t, $\rho_0 L$ for the fin line density ρ_1, $\rho_0 U_0^2$ for the Lagrangian momentum force and the penalty force $\boldsymbol{F_p}$, $\rho_0 U_0^2 L$ for the tension force ϕ and $\rho_0 U_0^2 L^3$ for the bending rigidity γ. The flexible fin motions were described by

$$\frac{\partial^2 \boldsymbol{X}}{\partial t^2} = \frac{\partial}{\partial s}\left(\phi\frac{\partial \boldsymbol{X}}{\partial s}\right) - \frac{\partial^2}{\partial s^2}\left(\gamma\frac{\partial^2 \boldsymbol{X}}{\partial s^2}\right) - \boldsymbol{F}+\boldsymbol{F_p}, \tag{3}$$

$$\frac{\partial \boldsymbol{X}}{\partial s}\cdot\frac{\partial \boldsymbol{X}}{\partial s} = 1, \tag{4}$$

where s is the Lagrangian coordinate along the fin and $\boldsymbol{X} = (X(s, t), Y(s, t))$ is the position. The penalty force $\boldsymbol{F_p}$ was only exerted on the leading edge of the flexible fin to be connected with the rigid head. The tension force ϕ was determined to satisfy the inextensibility condition in Eq. (4), whereas the bending rigidity γ was constant (Huang et al., 2007; Huang and Sung, 2010).

The motion of the circular rigid head was governed by

$$m_h\frac{\mathrm{d}^2\mathbf{X}_{h,c}(t)}{\mathrm{d}t^2} = -\int_{\Gamma_h}\mathbf{F}(s_h, t) - \boldsymbol{F}_p(t)\,\mathrm{d}s_h\,, \tag{5}$$

$$I_h\frac{\mathrm{d}^2\theta(t)}{\mathrm{d}t^2} = \tau_{pro} + \tau_F + \tau_{FP}, \tag{6}$$

where m_h is the head mass, $\boldsymbol{X}_{h,c}$ is the central position of the head, Γ_h is the head boundary, s_h is the arc-length along the head, I_h is the moment of inertia and θ is the rotation angle of the circular head. We used the characteristic scales $\rho_0 L^2$ and $\rho_0 L^4$ to define the units of the head mass m_h and the moment of inertial I_h, respectively. The external propulsion torque τ_{pro}, the torque from the fluid τ_F and the torque exerted by the penalty force $\boldsymbol{F_p}$ were obtained by

$$\begin{aligned}
&\tau_{pro} = A_{pro}\sin(2\pi ft),\\
&\tau_F = -\int_{\Gamma_h}\mathbf{R}(s_h, t)\times\mathbf{F}(s_h, t)\,\mathrm{d}s_h,\\
&\tau_{FP} = -\mathbf{R}(0, t)\times\mathbf{F}_P(t),
\end{aligned} \tag{7}$$